JOURNAL OF OPTOELECTRONICS AND ADVANCED MATERIALS Vol. 9, No. 6, June 2007, p. 1872 - 1877

Photoluminescence of Eu^{3+} and Sm^{3+} ions in SiO_2, SiO_2:Na_2O films formed from gels and ion implanted silica

J. C. PIVIN*, M. SENDOVA-VASSILEVA[a], G. LAGARDE[b], F. SINGH[c], A. PODHORODECKI[d], J. MISIEWICZ[d]
CSNSM-IN2P3, Bâtiment 108, 91405 Orsay Campus, France
[a]*CL SENES, Bulgarian Academy of Sciences, 72 Tzarigradsko Chaussee, 1784 Sofia, Bulgaria*
[b]*IPN, Bâtiment 100, 91405 Orsay Campus, France*
[c]*Nuclear Science Centre, Aruna Asaf Ali Marg, Post Box- 10502, New Delhi, India*
[d]*Institute of Physics, Wroclaw University of Technology, Wybrzeze Wyspianskiego 27, 50-370 Wroclaw, Poland*

Thin films of silica containing various concentrations of Eu^{3+} or Sm^{3+} ions were prepared by sol-gel chemistry and ion implantation for comparing the optical properties of these rare earth ions in both types of matrices after annealing. Sodium acetate was added in some of the gel films for investigating the changes in the crystal field and its influence on the RE emission. We found that the optimal temperature of annealing in air for the release of C and H from gels or defects from ion implanted silica, without segregating the rare earth, is of about 600 °C. The photoluminescence of Eu^{3+} and Sm^{3+} is enhanced significantly with the addition of Na in gels and the emission of Eu^{3+} becomes 20 times as intense as in silica implanted with the same concentration of Eu^{3+} ions.

(Received September 21, 2007; accepted April 26, 2007)

Keywords: Sol-gel, Rare earth, Luminescence

1. Introduction

The luminescence of rare earth ions (RE) finds numerous applications in display panels, television sets, lasers, amplifiers, etc [1-5]. However, an intense research effort is still devoted to the selection of suitable matrices for improving their emission efficiency. It is known that intra-4f transitions of free trivalent RE ions are generally spin forbidden. Electric dipole transitions become effective when the $^4f^n$ configuration is mixed with another having opposite parity (mainly $^4f^{n-1}$ 5d) under the effect of the ligand field [6]. Some are hypersensitive to the chemical environment [7]. The later may also be a source of quenching by re-absorption of the light, as for instance SiOH groups in silicate glasses or organic hydroxyl groups in gels [8]. Even when the chemical environment is favorable, the cross sections of optical absorption and radiative transitions remain often small, as for instance those of Sm^{3+} [9], Nd^{3+} [10], Er^{3+} [11]. Increasing the concentration of RE ions favors the luminescence quenching by up-conversion of excited states or by migration of these states between neighbor RE ions towards non radiative recombination centers. Moreover, the solubility of many RE in matrices useful for their compatibility with microelectronic technology and their optical transparency, such as SiO_2 and Al_2O_3, is less than 2 at% and they tend to segregate during thermal treatments, which are often needed for curing defects or eliminating impurities inherent in the synthesis procedure.

Sol-gel chemistry is the most versatile means for synthesizing oxide matrices with various compositions in order to tailor the refractive index, the ligand field and the solubility of RE ions. Lattice modifiers, such as Al, B or Pb can for instance be introduced in silica gel for increasing the solubility of RE [10, 12, 13]. Optical sensitizers can also be added to increase the effective absorption cross section or the electric field. That may be other dye ions, semiconducting nanoparticles with an exciton energy matching that of RE excited states [11, 14, 15] or noble metal particles enhancing the local electric field [16, 17]. However, a quenching of the luminescence of RE, especially Eu^{3+}, has often be reported in glasses derived from gels, because of the retention of C and H, even after annealing [8, 18]. It is also worth to note that investigations of the RE luminescence have been conducted mainly on gel monoliths, while thin films are more useful for applications as planar wave-guides integrated in circuits on silicon.

This paper reports a study of the $Eu^{3+}$and Sm^{3+} photoluminescence (PL) in silica films derived from gels and containing or not Na, as a function of the RE concentration and temperature of annealing. The PL is compared to that of same ions in more pure silica films, grown thermally, ion implanted with Eu or Sm. Na was added in the gel with the only purpose of ion exchanging Na with Ag, in order to obtain a matrix with an homogeneous and controlled spatial distribution of Ag clusters [19]. Indeed the direct addition of Ag salts in silica gel leads to the formation of metallic Ag aggregates. This second part of the investigation, the sensitization of the RE luminescence by Ag nanoparticles, will be the topics of another paper.

2. Experiment

The hydrolysis of tetraethoxysilane, $Si(OC_2H_5)_4$ (TEOS), was performed by addition of 2 moles of H_2O and 10^{-2} moles of HNO_3 per alkoxide mole, with stirring for 1h. Then $RENO_3.xH_2O$ diluted in ethanol was added to the TEOS sol in various proportions from 0.1 to 1 molar %. Sols containing 10 to 20 molar % of Na-$COOCH_3$ and 0.1 to 1 molar % of RE nitrate were also prepared. Films were deposited by spinning on Si wafers at a speed of 3000 rpm. After annealing, the composition and areal densities of atoms in all films were determined by Rutherford Backscattering Spectrometry (RBS) and their thickness calculated, using the atomic density of silica: the found values were of the order of 500 nm. The abbreviations T (TEOS without Na), TNa_1 (10 mol.% acetate) and TNa_2 (20 mol.% acetate) will be used in the following text and figures for the hydrolysed gel films and the oxide formed from these gel films by annealing in reference to the precursor.

Films of stoichiometric silica with a thickness of 500 nm (labelled S hereafter) were grown thermally on silicon wafers at 900°C. These films were implanted with 300 keV Eu^{2+} or Sm^{2+} ions at fluences of 10^{14} to 2×10^{15} cm^{-2}. According to SRIM calculations [20], these implantation conditions give a Gaussian depth distribution of RE ions peaking at 100 nm in silica, with a straggling of 30 nm and a concentration maximum of 0.02 to 0.4 at%. Implanted and annealed samples were characterized by RBS and these analyses showed that the actual depth profiles of Eu^{3+} or Sm^{3+} were very close to the calculated ones and remained unchanged after annealing.

The major defects in ion irradiated silica are E' centers, which are annealed at 600 °C [21, 22]. Therefore, implanted SiO_2 samples were annealed for 1h at 600 or 800 °C, in air, for repairing the host lattice. In the case of T samples, the annealing temperatures were increased up to 900°C in order to release as much H as possible and the treatments were performed in air for burning the residual C from ethoxy groups. Films were not annealed at temperatures higher than 900 °C to avoid the segregation of RE ions [15]. TNa samples were annealed at 600 or 800 °C in air for releasing hydrogen and carbon introduced in the gel, with a much higher concentration than in T samples, under the form of acetate. RBS analyses showed that Na starts to evaporate at 800 °C. The H contents of the films were measured by means of Elastic Recoil Detection Analysis (ERDA) under 3 MeV He^{2+} ion bombardment, and it was found that all gel films annealed in air at 600 °C contain 2 to 4 % H and those annealed at 800°C contain less than 0.5 at% H. The C contents were measured by means of the $^{12}C(d,p)^{13}C$ nuclear reaction (NRA). The found values are of the order of 2-4 at.% in as-deposited T films and of the order of 0.5-0.7%, 0.2-0.3% or 0.1% after annealing at 600 °C, 800 °C or 900 °C, respectively. The measured C concentrations in TNa_1 or TNa_2 annealed films are not much higher (1 or 2%, respectively, after annealing at 600 °C), probably because acetate groups are decomposed at low temperature. As discussed hereafter, this C contamination affects the luminescence properties, because C clusters, which are formed in SiOCH gels when the C concentration is sufficiently high [23, 24], emit in the same wavelength range than Eu^{3+} and Sm^{3+} ions.

The spectrometer used for the photoluminescence measurements consisted of a single grating monochromator with a resolution of 1 nm, coupled with a CCD camera as a detector. Spectra were not corrected for the spectral response of the camera, but all were recorded with the same window and no significant difference was recorded when shifting the window center from 600 to 650 nm. The light source was a Nd:YAG laser fitted with a Panther OPO, for splitting the pump photon into a pair of less energetic ones with wavelengths of 350 to 1000 nm. Series of emission spectra were recorded from selected samples with an excitation wavelength λ_{ex} increased by steps of 1 nm from 430 to 650 nm. The excitation curves of main Eu^{3+} and Sm^{3+} emissions were derived by plotting the respective peak heights as a function of λ_{ex}.

3. Results and discussion

The optical absorption and refraction of the matrix were analyzed by means of spectroscopic ellipsometry for a few T and TNa samples annealed at 600 °C. No significant absorption in the visible was observed with respect to pure silica, which means that very few defects have remained in the silica network and residual C or H atoms have no dramatic effect in this respect. Phase shifts could be fitted with the refractive index of silica and film thicknesses very close to those deduced from the independent analysis of Si and O concentrations by RBS and NRA ($^{16}O(d,p)^{17}O$ reaction).

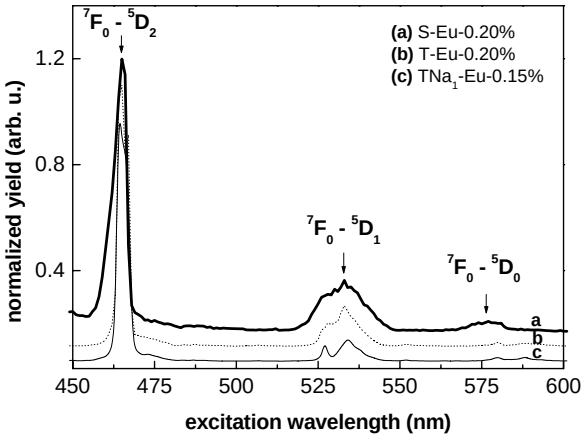

Fig. 1. Excitation curves of the Eu^{3+} emission at 610 nm in various matrices for Eu^{3+} atomic concentrations indicated in the figure. The implanted sample S-Eu^{3+} was annealed at 800°C while all gel samples were annealed at 600°C. The curves are normalized to the same intensity at the maximum. The spectra were shifted for clarity.

Three excitation peaks from the $^7F_0$ level of Eu^{3+} towards the $^5D_2$, $^5D_1$ and $^5D_0$ excited states, at 465, 530 and 580 nm respectively, can be identified in Fig. 1. Their relative heights are in good agreement with previously

reported absorption spectra [8]. Little differences are observed between the excitation spectra of Eu^{3+} in S, T and TNa samples in the spectral range from 430 to 650 nm, except that the $^7F_0$ - $^5D_0$ transition was observed only in spectra of S samples. Thus the Eu^{3+} emission spectra were recorded with excitation at 465 nm for comparing the emission yields as a function of the composition and the annealing temperature.

The strongest emission peak, at 610 nm, in emission spectra of all samples corresponds to the electric dipole transition between the $^5D_0$ excited state and the $^7F_2$ state of Eu^{3+} ions (Fig. 2). Weaker emission peaks at 580, 590, 650 and 700 nm are also intra-4f transitions: $^5D_0 \rightarrow {}^7F_0$, $^5D_0 \rightarrow {}^7F_1$ (magnetic transition), $^5D_0 \rightarrow {}^7F_3$, $^5D_0 \rightarrow {}^7F_4$ respectively as indicated in Fig. 2. The $^5D_0 \rightarrow {}^7F_J$ (J = 0 to 4) lines are overlapped by a broad emission band in spectra of annealed gel films, ascribed to the recombination of excitons in C clusters [23, 24]. The intensity ratio of this emission to that of $^5D_0 \rightarrow {}^7F_J$ lines of Eu^{3+} is maximum in the case of T samples annealed at 600°C. Note that the peak heights are normalized to a same maximum in Fig. 2 for comparing the peak shapes, so that the emission band of C clusters in spectra of TNa films cannot be seen because the $^5D_0 \rightarrow {}^7F_J$ peaks of Eu^{3+} are much more intense than in T samples. In the case of thermally grown films, there is no emission band simply because the C concentration is very low. Radiative transitions from higher excited states $^5D_1$ and $^5D_2$ of Eu^{3+} are not observed, indicating a very efficient non-radiative (multi-phonon) relaxation to the $^5D_0$ level, since in the absorption spectra excitation to both of these levels are observed. The magnetic dipolar transition, $^5D_0 \rightarrow {}^7F_1$ (λ_{em}=590 nm), and the two electric dipole transitions $^5D_0 \rightarrow {}^7F_3$ (λ_{em}=650 nm), $^5D_0 \rightarrow {}^7F_4$ (λ_{em}=700 nm) of Eu^{3+} are not observed in the spectra of SiO_2 implanted samples (Fig. 2). This difference is ascribed to a stronger coupling of 4f states in films derived from gels [6]. The main $^5D_0 \rightarrow {}^7F_2$ emission peak is slightly shifted in films containing Na ions, either because of a change in the local symmetry or in the intensity of the ligand field. The branching ratio of the $^5D_0 \rightarrow {}^7F_1$/$^5D_0 \rightarrow {}^7F_2$ lines, constitutes a sensitive probe of differences in the ligand field symmetry, since the $^5D_0 \rightarrow {}^7F_1$ magnetic dipolar transition is insensitive to the field symmetry, while the $^5D_0 \rightarrow {}^7F_2$ transition is hypersensitive to changes in the coupling factors between 4f states according to the environment [6-8]. The ratio F_1/F_2 is comparable in TNa samples (20±4 %) and T samples (24±3 %) annealed at 600° or 800 °C. More significant differences have been observed in more or less hydrolyzed gels by other authors [8, 18, 25]. The width of the $^5D_0 \rightarrow {}^7F_2$ peak is of about 20 nm in spectra of T samples annealed at 600 °C, whereas it is of 10 nm in all other samples (including T samples annealed at 800°C), and peaks recorded from T samples annealed at 600 °C show a shoulder on the high wavelength side, suggesting that a splitting of the F_2 peak might be observed with a better resolution. This result accounts for stronger fluctuations of ligand field in T samples annealed at 600 °C, due to its perturbation by impurities (H and C). The field around Eu^{3+} ions is less affected by these impurities in TNA samples annealed at same temperature, because of the stronger influence of Na^+ ions (reported hereafter).

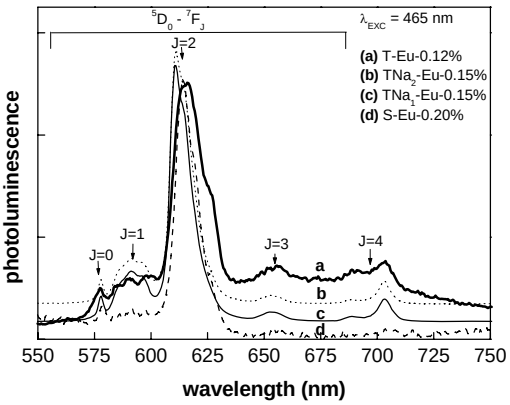

Fig. 2. Emission spectra of Eu^{3+} in various matrices, for Eu^{3+} concentrations indicated in the figure, normalized to the same intensity at the maximum for comparing their shapes. The implanted sample was annealed at 800 °C while gels samples were annealed at 600°C. Due to the normalization, the background related to the emission of carbon clusters appears less intense in the TNa_1 sample than in the T sample. The spectra were shifted for clarity.

The heights of the $^5D_0 \rightarrow {}^7F_2$ peaks were corrected for changes in the aperture of the spectrometer slits, source power, acquisition time and background of matrix emission, and have been used for comparing emission yields of Eu^{3+} ions as a function of the Eu^{3+} concentration, matrix and annealing temperature. In addition, the peak heights were divided by the number of Eu atoms per unit area in each sample, measured by RBS. The SiO_2 sample implanted with 2×10^{15} Eu ions/cm^2 annealed at 800°C has been taken as a reference. All emission yields per Eu atom were normalized to the emission yield of this sample. The measurement of $^5D_0 \rightarrow {}^7F_2$ peaks areas might have permitted a more quantitative estimation of relative emission yields, if there was no uncertainty due to the background in the case of T samples annealed at 600°C. For other films the ratios of peak areas and peaks heights are probably very close since they have same widths.

Table 1 presents the obtained results. A significant enhancement of the $^5D_0 \rightarrow {}^7F_2$ emission is observed in T samples annealed at 600°C compared to S samples annealed at same temperature, for Eu^{3+} concentrations in the range of 0.04 to 0.4 at.%. For T samples, it can be seen that the $^5D_0 \rightarrow {}^7F_2$ emission yield of Eu^{3+} ions decreases a little with the increase in Eu^{3+} concentration and more significantly with the increase in the annealing temperature. The quenching with the annealing temperature is stronger in silica films derived from gels free of Na than in thermally grown silica films. The emission yield of Eu^{3+} ions decreases by about a factor 15 to 20 in T films, instead of by a factor 1.4-1.5 in TNa and S films, when increasing the annealing temperature from 600 to 800 °C. This quenching may arise from a segregation of Eu^{3+} ions or from the migration of excited electrons between neighboring ions, then their transfer to a

defect. The segregation of Eu^{3+} ions is probably easier in silica gel films, because they are less dense than thermally grown films. On the other hand, the increase in the annealing temperature should induce a decrease in the number of defect states in films derived from gels and consequently an increase in the emission yield, since ion beam analyses (NRA, ERDA) show a loss of C and H. Since an opposite behavior is observed, Eu^{3+} ions probably segregate in gels films free of Na annealed at 800 °C and the Na addition seems to increase the solubility of Eu^{3+} ions.

The addition of 3.5 at.% Na into TEOS films (TNa_1) increases the $^5D_0 \rightarrow {}^7F_2$ emission yield by about a factor 6 for films annealed at 600 °C and 50 to 100 for those annealed at 800 °C (see Table 1). Since the branching ratio F_1/F_2 is not significantly affected by the Na addition, the enhancement of both Eu^{3+} emissions is more probably due to an increase in the degree of mixing of all 4f and 5d orbitals by the ligand field than to a modification of the field symmetry (and to an increase of Eu solubility for films annealed at 800 °C). We suppose that Eu^{3+} ions diffuse towards sites close to Na^+ ions in the glass network, where there is more free volume, and that their orbitals overlap more with O orbitals on these sites, because of the higher ionicity of Na-O bonds than of Si-O bonds. However, the comparison of emission yields in TNa_1 and TNa_2 films annealed at 600 °C, which undergo little loss of Na, shows that an increase of the Na concentration from 3.5 to 7 at.% leads to a decrease of the Eu^{3+} emission yield by about 30%. A more detailed investigation of the atomic environment of Na^+ and Eu^{3+} ions, using for instance EXAFS, and more accurate measurements of the O concentration by means of the $^{16}O(\alpha, \alpha)$ resonance would be useful for elucidating the causes of this effect. Indeed, we suppose that the O concentration in the glass decreases a little with the Na_2O concentration.

The absorption cross-sections of Sm^{3+} transitions in the visible are particularly weak [9]. However the excitation curves of the $^4G_{5/2} \rightarrow {}^6H_{7/2}$ (λ_{em} = 601-604 nm) and $^4G_{5/2} \rightarrow {}^6H_{9/2}$ (λ_{em}=650 nm) radiative transitions show several overlapping peaks in the range of 430 to 510 nm (see Fig. 3). The shapes of the excitation curves are similar for the two transitions, as shown for the TNa_1 sample in the figure. The peaks which are seen in the excitation curve of the ion implanted sample at 430, 455, 470, 487 and 505 nm are ascribed to transitions from the $^6H_{5/2}$ ground level to $^4I_{i/2}$ levels with i = 15, 13, 11, 9 and 7, respectively [6, 7, 9, 25]. More radiative de-excitation from the states with quantum numbers i=15, 13 and 7 is observed in ion implanted silica than in oxide films derived from gels. In the case of implanted silica, the $^4G_{5/2} \rightarrow {}^6H_{i/2}$ transitions can also be excited resonantly or by a cross relaxation process involving a transition from $^6H_{i/2}$ levels to the $^4G_{5/2}$ state [12], as evidenced by peaks at 550 and 600 nm in the excitation curve of the $^4G_{5/2} \rightarrow {}^6H_{9/2}$ emission (Fig. 3) or of the $^4G_{5/2} \rightarrow {}^6H_{7/2}$ emission (not shown). Sm^{3+} emission spectra were recorded with excitation at 487 nm for comparing the $^4G_{5/2} \rightarrow {}^6H_{i/2}$ emission yields as a function of the film composition and annealing treatment, because the excitation efficiency is close to its maximum at this wavelength in all studied films.

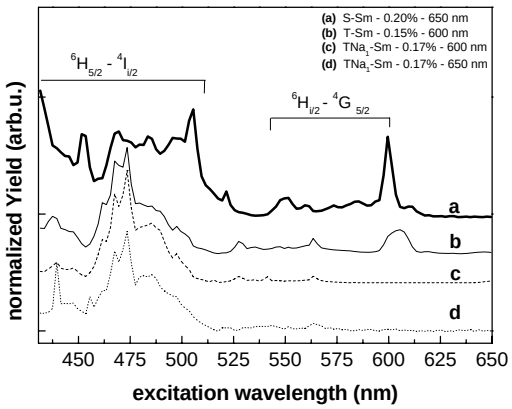

Fig. 3. Excitation curves of the Sm^{3+} emissions in various matrices for comparable Sm^{3+} concentrations indicated in the figure. S and T samples were annealed at 800°C while the TNa_1 sample was annealed at only 600 °C. The emission line, the yield of which was measured for obtaining these curves, is also indicated, but its shape depends little on the chosen emission because the excited level is the same. The curves are normalized to the same intensity in the maximum and vertically shifted for clarity.

Emission spectra of Sm^{3+} ions are shown in Fig. 4. The mean emission wavelengths, of 563-566 nm, 601-604 nm, 649-651 nm and 710 nm, of the $^4G_{5/2} \rightarrow {}^6H_{5/2}$, $^4G_{5/2} \rightarrow {}^6H_{7/2}$, $^4G_{5/2} \rightarrow {}^6H_{9/2}$ and $^4G_{5/2} \rightarrow {}^6H_{11/2}$ lines, respectively, are close to those reported by other authors for Sm^{3+} intra-4f transitions in silicate glasses [9, 25]. One can see that peaks recorded from the annealed gel films exhibit more splitting, due to fluctuations of the ligand field, and the branching ratios are somewhat different from those in implanted silica. The radiative transition from the $^4G_{5/2}$ to the $^6H_{9/2}$ state is the most probable in other types of samples, such as gels heated above 1000 °C [25] or SiO_2:Sm^{3+} co-sputtered films [26]. We observed that the branching ratio $^4G_{5/2} \rightarrow {}^6H_{7/2}$/ $^4G_{5/2} \rightarrow {}^6H_{9/2}$ changed for a same implanted sample with the annealing atmosphere (i.e. air or vacuum), and with aging of several weeks after the treatment. This ratio never exceeds 1 in spectra of S and T films annealed in air, but it can reach 2 in spectra of TNa films annealed in air. Its sensitivity to aging and to the annealing atmosphere seems to indicate that the de-excitation path is affected by minute changes in O or H concentration over depth ranges as large as 100 nm (which is the implantation mean range in the samples studied here). The mechanism may involve modifications of the local vibrational modes (Si-OH vibrations among others) or of the interaction between Sm^{3+} excited states and defects. The changes in O and H concentration could not be detected by means of NRA and ERDA. This aging constitutes a serious drawback to the use of Sm^{3+} as a light source in thin films for optoelectronic applications.

The PL yields were normalized as for samples containing Eu, using as a reference the SiO_2 sample implanted with 2×10^{15} Sm ions/cm^2 annealed at 800 °C.

We compared changes in the height of the $^4G_{5/2}\rightarrow{}^6H_{9/2}$ lines in the various samples and in the sum of the $^4G_{5/2}\rightarrow{}^6H_{i/2}$ (i = 5, 7, 9) peak areas. The normalized area is generally larger than the normalized height in gel films, but by a factor less than 2. We preferred to use the normalized heights of the $^4G_{5/2}\rightarrow{}^6H_{9/2}$ peaks for comparing emission yields in the different matrices, because the absolute intensity of this peak appears less sensitive to aging. Intensity ratios reported in Table 1 were measured a few days after annealing the samples. It can be seen in the table that the Sm^{3+} emission is stronger in S samples annealed at 600 °C than in the same samples annealed at 800 °C. The optimal temperature of annealing of SiO_2:Sm co-sputtered films for the PL of Sm^{3+} was also reported to be of 600 °C [26]. The PL yield decreases more with the Sm^{3+} concentration than in the case of Eu^{3+} ions, in SiO_2 samples annealed at 600° (above 0.10%) or 800°C (above 0.05%). These quenching effects with the increase in Sm^{3+} concentration or annealing temperature are also probably due to a segregation of Sm^{3+} ions. It is not possible to discriminate the Sm^{3+} emission peaks from that of C clusters in spectra of T samples annealed at 600 °C. One can only state that it is lower by more than 2 orders of magnitude than in pure silica films. The yield of the $^4G_{5/2}\rightarrow{}^6H_{9/2}$ transition is maximum in T samples annealed at 800 °C and re-decreases by a factor of 3 between 800 and 900 °C. Therefore, a compromise between the increasing tendency of Sm^{3+} ions to segregate and a more efficient release of impurities liable to quench the PL of Sm^{3+} ions seems to be reached at about 800 °C. The Sm^{3+} emission yield is larger in TNa samples annealed at 600 °C than in T samples annealed at same temperature. It is however 5 times less than in SiO_2 samples for the Na concentration of 3.5 at.% (Table 1) and 13 times for the Na concentration of 7 at.%. We conclude from these results that, as for Eu^{3+} ions, the modification of the ligand field induced by the addition of a limited concentration of Na increases the yield of the $^4G_{5/2}\rightarrow{}^6H_{y/2}$ transitions of Sm^{3+} ions (in the case of Sm^{3+} the Na addition also changes the branching ratio as discussed above). The PL of Sm^{3+} ions is however much more sensitive than that of Eu^{3+} to a quenching by a transfer of the excitation energy to defects or impurities, which are probably OH, CH_x groups retained in the oxide network or C clusters. As indicated by excitation curves shown in Fig. 3, some excitation paths of the Sm^{3+} luminescence are suppressed in oxide films formed from gels compared to thermally grown silica. The comparison of emission yields shows that the excitation is also less efficient at the optimal wavelength chosen for the experiments.

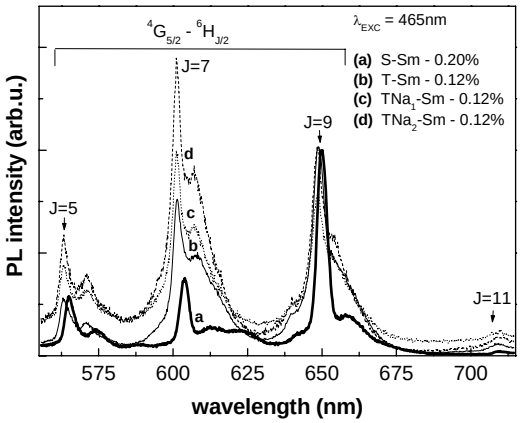

Fig. 4. Emission spectra of Sm^{3+} in various matrices, for Sm^{3+} concentrations indicated in the figure, normalized to the same intensity of the $^6H_{9/2}\rightarrow{}^4G_{5/2}$ transition for comparing their shapes. The Sm^{3+} emission in the T matrix annealed at 600 °C being overwhelmed by a background related to the emission of C clusters, the shown spectrum is that of a T sample annealed at 800 °C. The S and TNa_1 samples were annealed at 600 °C. The curves are vertically shifted for clarity.

Table 1. Normalized emission yields, measured with excitation at 465 nm for Eu^{3+} and 487 nm for Sm^{3+}, respectively. The presented values are normalized to the emission yield of the same ion in thermal silica (S) implanted with 2×10^{15} ions /cm^2 and annealed at 800 °C. Atomic concentrations are sorted under the form of intervals for limiting the number of columns, because they are never exactly the same in the sols and fluctuates of 10-20% with depth in some gel films.

Matrix-RE	T_{anneal}	0.02	0.04-0.06%	0.08-0.15%	0.20-0.25%	0.30-0.40%
S-Eu	600	2.0	1.8	1.5	1.3	1.5
S-Eu	800	1.2	1.3	1.2	1.3	1.0
T-Eu	600		7.0	6.0	5.8	4.6
T-Eu	800			0.39	0.24	0.20
TNa$_1$-Eu	600			38	35	36
TNa$_1$-Eu	800			22	20	25
TNa$_2$-Eu	600			25	22	
S-Sm	600	8.0	7.6	7.3	5.5	3.1
S-Sm	800	6.5	6.7	4.2	1.8	1.0
T-Sm	600	<0.05	<0.05	<0.05	<0.05	<0.05
T-Sm	800	3.3	3.1	3.1	1.5	0.73
T-Sm	900		1.2	1.1		
TNa$_1$-Sm	600			1.4	1.5	
TNa$_2$-Sm	600			0.55	0.50	

4. Conclusions

The optical properties of Eu^{3+} and Sm^{3+} embedded in silica-based matrices have been investigated as a function of the ions concentration, annealing temperature, matrix composition.

Whatever the matrix, the luminescence yield of Eu^{3+} ions decreases by less than a factor 2 with the Eu^{3+} concentration in the range of 0.02 to 0.40 at.%. It is quenched more by an increase of the annealing temperature from 600° to 800°C in the case of gels free of Na. The addition of Na into TEOS gels induces a significant enhancement of the luminescence yield of Eu^{3+} ions (by a factor of 6 to 100, depending on the annealing temperature), ascribed to an increase in the ligand field strength and Eu solubility. The sol-gel matrix appears to be a better host than pure silica for Eu^{3+} ions. The decrease of the emission yield with the annealing temperature and Eu^{3+} concentration is ascribed to a segregation process.

The impurities retained in glass films formed from gels have a stronger quenching effect on the Sm^{3+} emission than in the case of Eu^{3+}, since the emission yield in annealed silica-gel samples, with or without Na, is weaker than in ion implanted silica. However, the addition of Na improves also the emission of Sm^{3+} ions.

Acknowledgments

The authors are thankful to G. Salczer of CEA, Saclay, for experiments of spectroscopic ellipsometry and the spectra processing. This research work was made possible with the financial support of the PECO project 12530, concerning the collaboration of CSNSM and SENES, and of the IFPCAR project 2808-3, concerning that of CSNSM and NSC and POLLONIUM project, concerning the collaboration of CSNSM and IP-WUT.

References

[1] C. L. Pope, B. R. Reddy, S. K. N. Stevenson. Opt. Lett. **22**, 295 (1997),
[2] R. A. McFarlane. J. Opt. Soc. Am. **B 11**, 871 (1994).
[3] H. E. Heidepriem, W. Seeber, D. Ehrt. J. Non-Cryst. Solids **183**, 191 (1995).
[4] M. Dejneka, E. Snitzer, R. E. Riman. J. Non-Cryst. Solids **202**, 23 (1996).
[5] M. Naftaly, A. Jha, E. R. Taylor. J. Non-Crystal. Solids **256&257**, 248 (1999).
[6] R. D. Peacock, In J. D. Dunitz, ed.: Structure and Bonding **22**, 83 (Springer Verlag, 1975).
[7] R. Reisfeld, C. K. Jorgensen. In K. A. Gschneidner, L. Eyring, ed.: Handbook of physics and chemistry or rare earths **9**, Chapt. 58, pp 1-40 (North Holland, Amsterdam, 1987.
[8] D. Hreniak, M. Jasiorski, K. Maruszewski, L. Kepinski, L. Krajczyk, J. Misiewicz, W. Strek. J. Non-Crystal Solids **298**, 146 (2002).
[9] K. Annapurna, R.N. Dwivedi, A. Kumar, A. K. Chaudhuri, S. Buddhudu. Spectrochimica Acta part A **56**, 103 (1999).
[10] M. Langlet, C. Coutier, W. Meffre, M. Audier, J. Fick, R. Rimet, B. Jacquier. J. Lumin. **96,** 295 (2002).
[11] G. Franzo, F. Iacona, V. Vincigueiro, F. Priolo. Mat. Sci. Engineer. **B69**, 3**35** (2000).
[12] C. Armellini, M. Ferrari, M. Montagna. J. Non-Crystal. Solids **245**, 115 (1999).
[13] A. Patra, R. Reisfeld, H. Minti. Materials Lett. **37**, 325 (1998).
[14] A. Chasera. J. Sol-Gel Sci. and Technol**. 26,** 943 (2003).
[15] M. Jimenez de Castro, J.C. Pivin, J. Sol-Gel Sci. and Technol. **28**, 37 (2003).
[16] O. L. Malta, M. A. Couto dos Santos, Chem. Physics Letters **174**, 13 (1990).
[17] T. Hayakawa, S. T. Selvan, M. Nogami. J Non-Crystal Solids **259**, 16 (1999).
[18] C. McDonagh, G. Ennis, P. Marron, B. O'Kelly, Z. R. Tang, J.F. McGilp. J. Non-Crystal Solids **147**, 97 (1992).
[19] J. C. Pivin. In functional properties of nanostructured materials, eds. R. Kassing, P. Petkov, W. Kulish, C. Popov, NATO Science Series II: Mathematics, Physics and Chemistry, **223**, Springer, Dortrecht, Netherlands (2006), ISBN: 1-4020-4593-X].
[20] J. P. Biersack. Nucl. Instr. and Meth**. B 27**, 21 (1987).
[21] A. H. Edwards. Nucl. Instr. and Meth. **B 32**, 238 (1988).
[22] L. Rebohle. Appl. Phys. Lett. **71**, 2809 (1997).
[23] J. C. Pivin, M. Sendova-Vassileva. Solid State Commun. **106**, 133 (1998).
[24] J. C. Pivin, P. Colombo, A. Martucci, G. D. Soraru, E. Pippel, M. Sendova-Vassileva. J. Sol-Gel Sci. and Technol. **26**, 251 (2003).
[25] R. Reisfeld, M. Zelner, A Patra. J. Alloys and Compounds **300**, 147 (2000).
[26] M. Sendova-Vassileva, A. Vuchkov, O. Angelov, D. Dimova-Malinovska, J. C. Pivin. J. Mat. Sci: Mat. in Electronics **14**, 853 (2003).

*Corresponding author: jc.pivin@club-internet.fr